
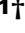








Interleukin-23 receptor expressing $\gamma\delta$ T cells locally promote early atherosclerotic lesion formation and plaque necrosis in mice

Jesus Gil-Pulido ^{1†}, Núria Amézaga ^{1†}, Ivana Jorgacevic ^{1†}, Helga D. Manthey¹, Melanie Rösch¹, Theresa Brand ², Peter Cidlinsky ¹, Sarah Schäfer ¹, Andreas Beilhack ³, Antoine-Emmanuel Saliba⁴, Kristina Lorenz ^{2,5}, Louis Boon⁶, Immo Prinz^{7,8}, Ari Waisman ⁹, Thomas Korn ^{10,11,12}, Clément Cochain ^{1,13}, and Alma Zernecke ^{1*}

¹Institute of Experimental Biomedicine, University Hospital Würzburg, Josef-Schneider-Str. 2, 97078 Würzburg, Germany; ²Institute of Pharmacology and Toxicology, University of Würzburg, Versbacher Straße 9, 97078 Würzburg, Germany; ³Department of Internal Medicine II, University Hospital Würzburg, Zinklesweg 10, 97078 Würzburg, Germany; ⁴Helmholtz Institute for RNA-based Infection Research (HIRI), Helmholtz-Center for Infection Research (HZI), Josef-Schneider-Straße 2, 97080 Würzburg, Germany; ⁵Leibniz-Institut für Analytische Wissenschaften—ISAS-e.V., Bunsen-Kirchhoff-Straße 11, 44139 Dortmund, Germany; ⁶JJP Biologics, Bobrowiecka 8, 00-728, Warsaw, Poland; ⁷Institute of Systems Immunology, University Medical Center Hamburg Eppendorf, Martinistr. 52, 20246 Hamburg, Germany; ⁸Institute of Immunology, Hannover Medical School, Carl-Neuberg-Str. 1, 30625 Hannover, Germany; ⁹Institute for Molecular Medicine, and Research Center for Immunotherapy, University Medical Center of the Johannes Gutenberg-University Mainz, Langenbeckstraße 1, 55131 Mainz, Germany; ¹⁰Department of Neurology, Klinikum rechts der Isar, Technical University of Munich, Ismaninger Str. 22, 81675 Munich, Germany; ¹¹Institute of Experimental Neuroimmunology, Klinikum rechts der Isar, Technical University of Munich, Ismaninger Str. 22, 81675 Munich, Germany; ¹²Munich Cluster for Systems Neurology (SyNergy), Munich, Germany; and ¹³Comprehensive Heart Failure Center, Am Schwarzenberg 15, University Hospital Würzburg, 97080 Würzburg, Germany

Received 15 March 2021; editorial decision 21 November 2021; accepted 9 December 2021; online publish-ahead-of-print 13 December 2021

Time for primary review: 29 days

Aims

Atherosclerosis is a chronic inflammatory disease of the vessel wall controlled by local and systemic immune responses. The role of interleukin-23 receptor (IL-23R), expressed in adaptive immune cells (mainly T-helper 17 cells) and $\gamma\delta$ T cells, in atherosclerosis is only incompletely understood. Here, we investigated the vascular cell types expressing IL-23R and addressed the function of IL-23R and $\gamma\delta$ T cells in atherosclerosis.

Methods and results

IL-23R⁺ cells were frequently found in the aortic root in contrast to the aorta in low-density lipoprotein receptor deficient IL-23R reporter mice (*Ldlr*^{-/-}*Il23r*^{gfp/+}), and mostly identified as $\gamma\delta$ T cells that express IL-17 and GM-CSF. scRNA-seq confirmed $\gamma\delta$ T cells as the main cell type expressing *Il23r* and *Il17a* in the aorta. *Ldlr*^{-/-}*Il23r*^{gfp/gfp} mice deficient in IL-23R showed a loss of IL-23R⁺ cells in the vasculature, and had reduced atherosclerotic lesion formation in the aortic root compared to *Ldlr*^{-/-} controls after 6 weeks of high-fat diet feeding. In contrast, *Ldlr*^{-/-}*Tcrδ*^{-/-} mice lacking all $\gamma\delta$ T cells displayed unaltered early atherosclerotic lesion formation compared to *Ldlr*^{-/-} mice. In both HFD-fed *Ldlr*^{-/-}*Il23r*^{gfp/gfp} and *Ldlr*^{-/-}*Tcrδ*^{-/-} mice a reduction in the plaque necrotic core area was noted as well as an expansion of splenic regulatory T cells. *In vitro*, exposure of bone marrow-derived macrophages to both IL-17A and GM-CSF induced cell necrosis, and necroptotic RIP3K and MLKL expression, as well as inflammatory mediators.

Conclusions

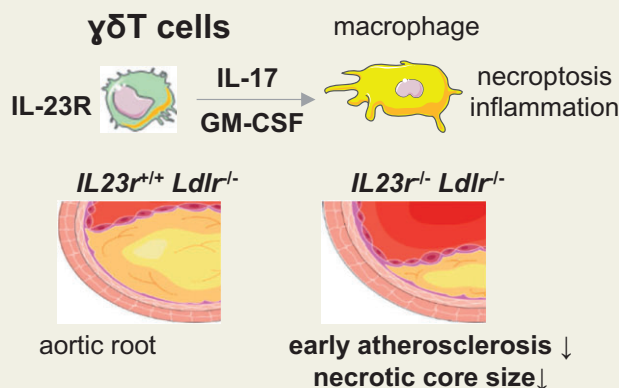
IL-23R⁺ $\gamma\delta$ T cells are predominantly found in the aortic root rather than the aorta and promote early atherosclerotic lesion formation, plaque necrosis, and inflammation at this site. Targeting IL-23R may thus be explored as a therapeutic approach to mitigate atherosclerotic lesion development.

*Corresponding author. Tel: +49 (0) 931 201 48331; fax: +49 (0) 931 201 648341, E-mail: alma.zernecke@uni-wuerzburg.de

[†]The first three authors contributed equally to the study.

Published on behalf of the European Society of Cardiology. All rights reserved. © The Author(s) 2021. For permissions, please email: journals.permissions@oup.com.

Graphical Abstract



Keywords

Atherosclerosis • Inflammation • Lymphocyte • T cells

1. Introduction

Atherosclerosis is a chronic inflammatory disease of the vessel wall driven by the progressive intimal accumulation of leucocytes. It is well recognized that immune responses play a critical role in atherogenesis.^{1,2} Monocytes differentiate into macrophages and take up oxidized LDL (oxLDL) to transform into foam cells. The apoptosis of foam cells and other leucocytes eventually overwhelms the phagocytic capacities of viable macrophages, and necrosis leads to the formation of a lipid-rich, highly proinflammatory necrotic core. In addition, proinflammatory programmed cell necrosis, or necroptosis, promotes the growth of the necrotic core.^{1–3} Also adaptive immune responses are activated, and a balance between proinflammatory and regulatory T-cell (Treg) responses control atherosclerosis.⁴ Among CD4⁺ T cells, interferon (IFN)- γ producing T-helper 1 (Th1) cells promote atherosclerosis, Th2 responses contribute to atheroprotection or protection, dependent on the context and model, and Foxp3⁺CD25⁺ Tregs inhibit vascular inflammation. The function of IL-17 is still controversial,⁴ likely related to different IL-17-expressing cell types, which include Th17 cells and $\gamma\delta$ T cells. $\gamma\delta$ T cells are found in healthy vessels and in the aortic root in mice and humans.^{5,6} The absence of $\gamma\delta$ T cells, however, has not been found to affect lesion formation in apolipoprotein E-deficient (*ApoE*^{-/-}) mice.^{7,8}

IL-23 receptor (IL-23R) is mainly expressed by Th17 cells and $\gamma\delta$ T cells.⁹ The IL-23R is regarded as the only signal-transducing component of the IL-23R: IL-12R β 1 complex and binds the α -chain (p19) of IL-23, which unlike the β -chain (p40) of IL-23 interacting with IL-12R β 1 is not shared with IL-12.¹⁰ In Th17 cells, IL-23 promotes a pathogenic Th17 phenotype characterized by the expression of IL-17, GM-CSF, and IFN- γ ,^{11,12} as opposed to non-pathogenic Th17 cells expressing IL-17 and IL-10.^{13,14} Similarly, pathogenic effector $\gamma\delta$ T cells that express IL23R, IL-17, and GM-CSF have been described in experimental autoimmune encephalomyelitis.^{15–17}

The role of IL-23/IL-23R in atherosclerosis is controversial. Administration of recombinant IL-23 promoted plaque necrosis and macrophage apoptosis in atherosclerosis-prone low-density lipoprotein receptor knockout (*Ldlr*^{-/-}) mice,¹⁸ but *Ldlr*^{-/-} mice deficient in IL-23R

did not show alterations in atherosclerotic lesion development or phenotype upon 10 weeks of high-fat diet (HFD) feeding.¹⁹ At advanced stages of lesion formation after 16 weeks of Western diet, deficiency in IL-23 increased lesion formation in the aortic root of *Ldlr*^{-/-} mice by deterioration of the intestinal barrier and expansion of pro-atherogenic bacteria and metabolites.²⁰

Notably, IL-23R-dependent $\gamma\delta$ T cells are found in the aortic root,⁶ and overexpression of IL-23 has been shown to cause inflammation within the aortic sinus by acting on IL23R⁺CD3⁺CD4⁺CD8⁻ cells,²¹ presumably $\gamma\delta$ T cells. $\gamma\delta$ T cells within tissues can respond via antigen-dependent but also antigen-independent mechanisms that allow them to rapidly activate specific effector functions.^{22,23} IL23R expressing $\gamma\delta$ T cells may thus be of particular importance for promoting early vascular inflammation and atherosclerotic lesion formation, not investigated previously, rather than lesion growth.

Therefore, we here set out to characterize IL-23R⁺ cells, and investigate the function of IL-23R and $\gamma\delta$ T cells particularly during early atherogenesis. To this end, we used mice with a knock-in of green fluorescent protein (GFP) into the endogenous *Il23r* gene⁹ to investigate IL-23R expression on immune cells based on the detection of GFP in heterozygous *Il23r^{gfp/+}* mice still fully responsive to IL-23, and its function in *Il23r^{gfp/gfp}* mice lacking functional IL-23R, crossed with atherosclerosis-prone *Ldlr*^{-/-} mice. Moreover, we investigated also δ TCR-deficient (*Tcr δ ^{-/-}*) *Ldlr*^{-/-} mice that lack $\gamma\delta$ T cells. We uncovered $\gamma\delta$ T cells to be the predominant cell type expressing IL-23R within aortic tissue, and IL-23R⁺ $\gamma\delta$ T cells to produce IL-17A and GM-CSF. Disruption of IL-23R signalling inhibited early lesion development and reduced necrotic core size locally in aortic root lesions, demonstrating that IL-23R⁺ $\gamma\delta$ T cells play a role in promoting early atherosclerosis and plaque necrosis.

2. Methods

A detailed version of materials and methods appears in the [Supplementary material online](#).

2.1 Mice and diet

IL-23R-GFP knock-in mice were generated by introducing an internal ribosome entry site-GFP-cassette into the endogenous *Il23r* gene.⁹ Whereas heterozygous *Il23r^{gfp/+}* mice can be used as reporter mice to identify IL-23R-expressing GFP⁺ cells (fully responsive to IL-23 because of the intact *Il23r* allele), homozygous *Il23r^{gfp/gfp}* mice are unresponsive to IL-23 due to two mutated *Il23r* alleles. *Ldlr^{-/-}* mice (The Jackson Laboratory) were crossed with *Il23r^{gfp/+}* mice to generate *Ldlr^{-/-}*, *Ldlr^{-/-}Il23r^{gfp/+}* and *Ldlr^{-/-}Il23r^{gfp/gfp}* mice (C57BL/6 background), and with *Tcrδ^{-/-}* mice (The Jackson Laboratory) to generate *Ldlr^{-/-}* and *Ldlr^{-/-}Tcrδ^{-/-}* mice (C57BL/6 background). To induce atherosclerosis, male and female mice aged between 6 and 8 weeks were placed on a HFD (15% milk fat, 1.25% cholesterol, Altromin). Animals were euthanized by an overdose of isoflurane anaesthesia (5% concentration), and subsequent exsanguination and organ isolation. All animal studies conform to the Directive 2010/63/EU of the European Parliament and have been approved by the appropriate local authorities (Regierung von Unterfranken, Würzburg, Germany).

2.2 Flow cytometry

Fat was removed from the aorta, and the aorta was separated from the aortic root. They were each minced and enzymatically digested, and cells were stained with specific antibodies. Dead cells were removed from the analysis. Intracellular staining was performed in cells treated with brefeldin A, and ionomycin. To co-detect intracellular cytokines in *Il23r^{gfp/+}* mice, cells were fixed after surface staining using 2% formaldehyde to retain GFP expression before intracellular staining. Bone marrow-derived macrophages (BMDMs) were stained using the AnnexinV Apoptosis Detection Kit (ThermoFisher, Scientific). Probes were analysed using a FACSCantoll or FACSCelesta and FlowJo 10.0 software (BD Biosciences).

2.3 Two-photon imaging

Aortic roots were imaged using an upright two-photon fluorescence microscope (TCS SP8 MP, Leica).

2.4 Immunohistochemistry and atherosclerotic lesion quantification

Arteries were perfusion-fixed *in situ* with phosphate buffered saline (PBS) followed by 4% paraformaldehyde (PFA) in PBS. The heart was removed for post-fixation in 4% PFA. The heart was embedded in Tissue Tek, frozen, and cut into 5 µm transverse sections. Aortic root sections were collected when all three valves were clearly visible. Three sections, 75 µm apart were stained by haematoxylin–eosin, and the average atherosclerotic plaque size was quantified. Quantification of plaque size in the aorta was performed after staining lipid depositions using Oil-Red-O. The area of the aorta occupied by Oil-Red-O⁺ lipids was quantified by computerized image analysis (Diskus Software), expressed as the percentage of total aortic area. Sections through the aortic root were used for immunofluorescence staining. Necrotic core formation was quantified in sections stained with haematoxylin and eosin by measuring lightly stained plaque area devoid of haematoxylin-stained cell nuclei. Apoptotic cells were detected by TUNEL. Images were recorded with a Leica DM 4000B fluorescence microscope and JVC KY-F75U camera. Plaque size and cell content were quantified by computerized image analysis (Diskus Software, Hilgers) and by investigators blinded to the group distributions.

2.5 Serum cholesterol measurement

Total cholesterol was analysed in serum (Amplex Red Cholesterol Assay Kit, Invitrogen).

2.6 Quantitative PCR analysis

Total RNA was isolated, reverse transcribed into cDNA, and quantitative real-time polymerase chain reaction (PCR) analysis was performed using SYBR-Green and specific primer pairs (QuantiStudio6 Flex Thermal Cycler, Applied Biosystems).

2.7 Bone marrow-derived antigen-presenting cells and BMDMs

Bone marrow cells were cultured in media containing 20 ng/mL GM-CSF (PeproTech) to obtain bone marrow-derived antigen-presenting cells (BM-APCs), and 15% L-929 cell-conditioned medium to obtain BMDMs.

2.8 CITE-seq analysis of total cells from mouse aortas

Circulating leucocytes were excluded from the analysis by injecting anti-CD45.2 intravenously before sacrifice. Aortas were enzymatically digested and cells were labelled with cellular indexing of transcriptomes and epitopes by sequencing (CITE-seq) and hashtag antibodies. Cells were sorted, counted in Trypan blue (>85% viability), and loaded in the 10× Genomics Chromium (Single Cell 3' v3 reagents, 10× Genomics) and scRNA-seq, ADT, and HTO libraries were prepared.²⁴ After sequencing (Novaseq 6000 platform, Illumina), data were demultiplexed using Cell Ranger software v3.1.0. Mouse mm10-3.0.0 reference genome was used for alignment. Cell surface proteins were evaluated using feature-ref flag of Cell Ranger software. Cell Ranger gene-barcode matrix was analysed using Seurat v3, and clustering was performed using the 'FindClusters' function. Mononuclear phagocytes and fibroblast subclusters were manually pooled to facilitate data visualization in Figure 1.

2.9 Western blot

Cell lysates were subjected to SDS-PAGE and blotted onto nitrocellulose. Membranes were blocked, incubated with primary/secondary antibody, and developed using enhanced chemiluminescence reagent. Images were recorded (Amersham Imager 600) and quantified (ImageQuantTL software, GE Healthcare).

2.10 Statistical analysis

Data represent mean ± SD. Comparisons were performed via unpaired Student's *t*-test, one-way, two-way or three-way ANOVA followed by a Tukey's multiple comparison test using Prism software (GraphPad). Differences were considered statistically significant at *P* < 0.05.

3. Results

3.1 γδ T cells are the major cell population expressing IL-23R within the aortic sinus

Previous studies have shown that mice overexpressing IL-23 develop inflammation in the aortic root, the presence of IL-23R⁺ CD3⁺CD4⁻CD8⁻ T cells at this site,²¹ and that γδ T cells can be identified in the aortic root by immunofluorescence staining in *Tcrδ-H2BeGFP* reporter mice.⁶ Using IL-23R reporter mice (*Il23r^{gfp/+}*) crossed with *Ldlr^{-/-}* mice, we found GFP-expressing IL-23R⁺ cells to represent ~3% of total CD45⁺ cells in the aorta and up to ~10% of leucocytes in the aortic

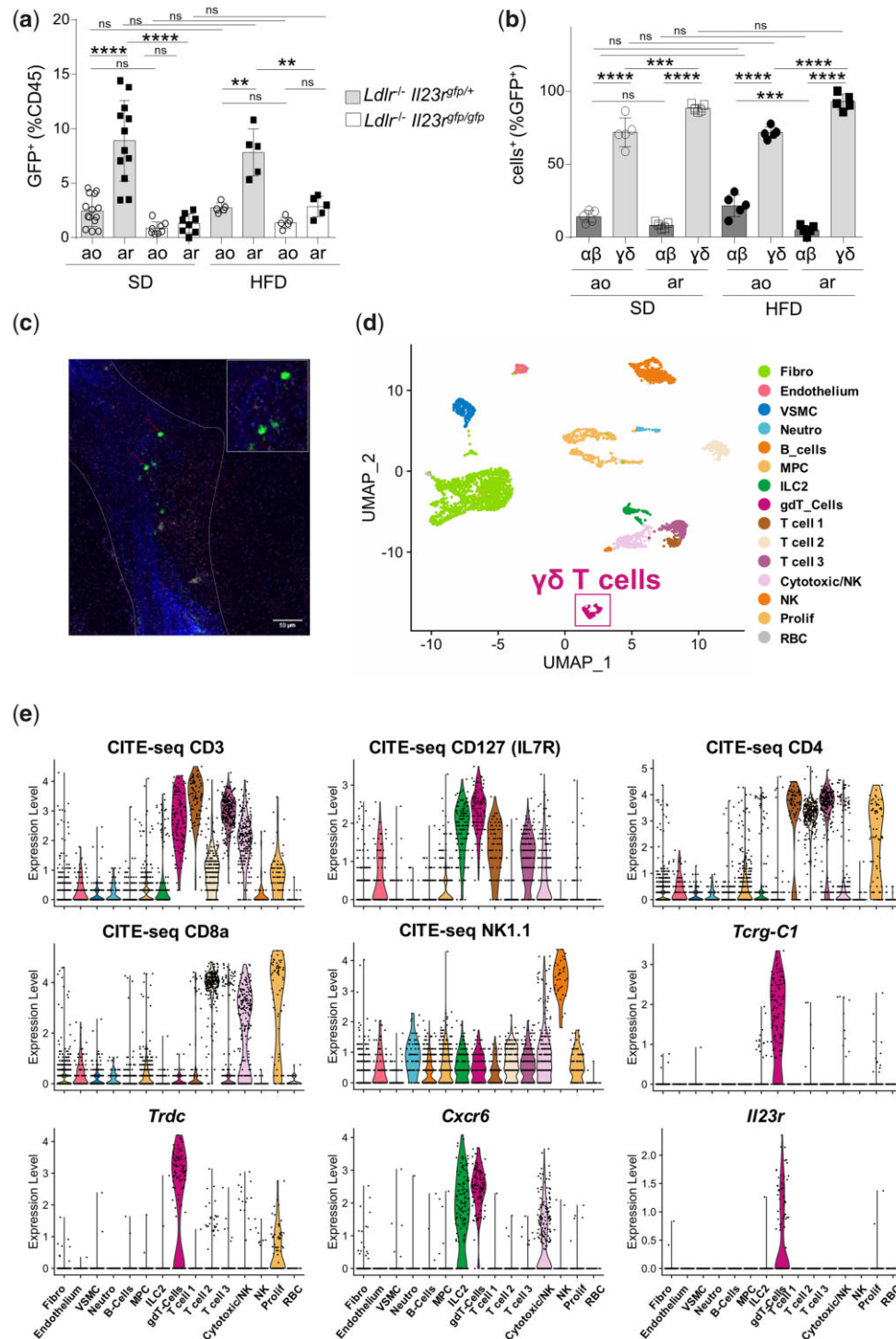


Figure 1 IL-23R is expressed by $\gamma\delta$ T cells. (A and B) Aortas (ao) and aortic roots (ar) from mice fed a SD or HFD were analysed by flow cytometry. (A) Percentages of GFP⁺ cells among CD45⁺ cells in *Ldlr*^{-/-}*Il23r*^{gfp/+} (*n* = 12, SD; *n* = 5, HFD) and *Ldlr*^{-/-}*Il23r*^{gfp/gfp} (*n* = 8, SD; *n* = 5, HFD) mice are shown. (B) Percentages of $\gamma\delta$ and $\alpha\beta$ T cells among GFP⁺ cells in *Ldlr*^{-/-}*Il23r*^{gfp/+} (*n* = 5 in all conditions) mice are shown. Data is presented as a mean ± SD. Statistical significance was determined by three-way ANOVA. ***P* < 0.01, ****P* < 0.001, *****P* < 0.0001; ns, non-significant. (C) Localization of GFP⁺ cells in the aortic root of a *Ldlr*^{-/-}*Il23r*^{gfp/+} mouse by two-photon microscopy; dashed lines mark the aortic root circumference; scale bar, 50 μ m. (D) CITE-seq was performed on the aorta obtained from *Ldlr*^{-/-} mice (*n* = 5 pools of 2 aortas) after 13 weeks of HFD. A total of 4058 single-cell transcriptomes are represented using an UMAP plot. Using marker genes, cells are assigned and colour-coded to clusters with labelled identities. Fibro, fibroblasts; VSMC, vascular smooth muscle cells; Neutro, neutrophils; MPC, mononuclear phagocytes; ILC2, innate lymphoid cells type 2; gdT, gammadelta T cells; NK, natural killer cells; prolif, proliferating cells; RBC, red blood cells. (E) Violin plots depicting log normalized expression of indicated cell surface markers (as measured by CITE-seq) and transcripts in the cell populations; Colour-code as in panel (D).

root in 8 week old mice fed a standard diet (SD) (Figure 1A). Similar frequencies were observed in mice upon feeding a HFD for 6 weeks (Figure 1B). Although a significant increase in leucocytes was observed in the aorta of *Ldlr*^{-/-} mice and cell numbers tended to be increased in the aortic root of *Ldlr*^{-/-}, *Il23r*^{gfp/+} *Ldlr*^{-/-}, and *Il23r*^{gfp/gfp} *Ldlr*^{-/-} mice after HFD-feeding, absolute counts of IL-23R⁺ cells were unaltered in the aorta and the aortic root in SD compared to HFD-fed *Il23r*^{gfp/+} *Ldlr*^{-/-} and *Il23r*^{gfp/gfp} *Ldlr*^{-/-} mice in the aortic root (Supplementary material online, Figure S1a and b). In the aortic root and aorta, ~90% and ~70% of GFP⁺ cells could be identified as $\gamma\delta$ T cells, respectively; the remaining cells corresponded to conventional $\alpha\beta$ T cells in both SD and HFD-fed *Il23r*^{gfp/+} *Ldlr*^{-/-} mice (Figure 1B, Supplementary material online, Figure S2). $\gamma\delta$ T cells amounted to ~10% of leucocytes in the aortic root but only ~2.5% of total CD45⁺ cells in the aorta in mice fed a SD or HFD (Supplementary material online, Figure S1c). Approximately 95% of $\gamma\delta$ T cells present in the aortic root showed expression of IL-23R in contrast to ~75% $\gamma\delta$ T cells in the aorta, irrespective of diet (Supplementary material online, Figure S1d). IL23R⁺ $\gamma\delta$ T cells were also frequently detected in the aortic root of *Il23r*^{gfp/+} *Ldlr*^{-/-} mice by multiphoton microscopy (Figure 1C). Additionally, we explored the cell types expressing *Il23r* transcripts by scRNA-seq (10 \times Genomics v3 reagents) and CITE-seq²⁵ of total viable cells in atherosclerotic aortas from *Ldlr*^{-/-} mice fed a HFD for 13 weeks. *Il23r* transcripts were exclusively detected in a cluster of $\gamma\delta$ T cells defined as CD3⁺CD127⁺CD4⁻CD8a⁻NK1.1⁻ cells expressing T-cell receptor delta, constant region, T-cell receptor gamma, constant 1, and C-X-C chemokine receptor type 6 (*Cxcr6*) (Figure 1D and E). In previously generated datasets of aortic CD45⁺ leucocytes,^{24,26,27} *Il23r* transcripts were detected in a cluster of Cd3d⁺Cd4⁻Cd8b1⁻*Cxcr6*⁺ innate like T cells, consistent with $\gamma\delta$ T cells, both in non-atherosclerotic and atherosclerotic aortas (Supplementary material online, Figure S3, transcripts encoding T-cell receptor delta and gamma chain were not detected in these data generated using 10 \times Genomics v2 reagents).

Deficiency in IL-23R entailed a loss in relative proportions of IL-23R⁺ cells in the aortic root both in SD and HFD-fed in *Ldlr*^{-/-} *Il23r*^{gfp/gfp} mice compared to frequencies in *Ldlr*^{-/-} *Il23r*^{gfp/+} mice (Figure 1A). Residual IL-23R⁺ cells in *Ldlr*^{-/-} *Il23r*^{gfp/gfp} mice were conventional $\alpha\beta$ T cells (Supplementary material online, Figure S1e). Taken together, these results show that substantially higher frequencies of IL-23R⁺ cells are found in the aortic root compared to the aorta. These IL-23R⁺ cells primarily constitute $\gamma\delta$ T cells, which do not expand in atherosclerosis and require IL-23R for their maintenance.

3.2 IL23R⁺ $\gamma\delta$ T cells in the atherosclerotic aortic root produce IL-17A and GM-CSF

We further characterized the cytokine expression profile of these vascular IL-23R-expressing $\gamma\delta$ T cells in aortic root digests after *in vitro* stimulation with PMA, brefeldin and ionomycin by flow cytometry. As expected, the majority of IL23R⁺ $\gamma\delta$ T cells produced IL-17A and to a lesser extent also GM-CSF. IFN- γ was expressed in single $\gamma\delta$ T cells (0–3%) and mostly confined to IL23R⁻ $\alpha\beta$ ⁺ T cells that did not express IL-17 or GM-CSF (Figure 2A–C and Supplementary material online, Figure S2). Analysis of scRNA-seq data of aortic cells was consistent with these results, with $\gamma\delta$ T cells being enriched for *Il17a* and rarely presenting detectable *Ifng* transcripts. GM-CSF (*Csf2*) was mostly enriched in adventitial type 2 innate lymphoid cells (ILC2s),²⁸ but transcripts were also detected in $\gamma\delta$ T cells (Supplementary material online, Figure S3c and d). Upon HFD-feeding for 6 weeks, IL-17A expression was unaltered in

IL-23R⁺ $\gamma\delta$ T cells in *Ldlr*^{-/-} *Il23r*^{gfp/+} mice and was increased in the few remaining IL-23R⁺ $\gamma\delta$ T cells in *Ldlr*^{-/-} *Il23r*^{gfp/gfp} mice (Figure 2D). We also noted a significant increase in GM-CSF production in IL-23R⁺ $\gamma\delta$ T cells in *Ldlr*^{-/-} *Il23r*^{gfp/+} mice with HFD-feeding, and frequencies of GM-CSF⁺ IL23R⁺ $\gamma\delta$ T cells were lower in diet-fed *Ldlr*^{-/-} *Il23r*^{gfp/gfp} compared to *Ldlr*^{-/-} *Il23r*^{gfp/+} mice (Figure 2E). In line with the loss of IL-23R⁺ cells in *Ldlr*^{-/-} *Il23r*^{gfp/gfp} mice, frequencies of IL-17A-producing GFP⁺ $\gamma\delta$ T cells among total leucocytes were markedly reduced in SD and HFD-fed IL-23R-deficient *Ldlr*^{-/-} *Il23r*^{gfp/gfp} mice compared to *Ldlr*^{-/-} *Il23r*^{gfp/+} mice (Figure 2G), and GM-CSF-producing GFP⁺ $\gamma\delta$ T cells were lower in HFD-fed *Ldlr*^{-/-} *Il23r*^{gfp/gfp} mice (Figure 2H). When separately analysing the capacity of $\gamma\delta$ T cells to secrete both of these cytokine, we observed an expansion of IL-17A⁺GM-CSF⁺ double positive IL-23R⁺ $\gamma\delta$ T cells in HFD-fed *Ldlr*^{-/-} *Il23r*^{gfp/+} mice, and again a loss in IL-17A⁺GM-CSF⁺IL-23R⁺ $\gamma\delta$ T cells among CD45⁺ leucocytes was seen in both SD and HFD-fed *Ldlr*^{-/-} *Il23r*^{gfp/gfp} mice (Figure 2J–L). There were no major changes in IFN- γ production within $\alpha\beta$ or $\gamma\delta$ T cells (Figure 2F), but increased frequencies of IFN- γ ⁺ $\alpha\beta$ ⁺ T cells among total leucocytes were noted in HFD compared to SD-fed *Ldlr*^{-/-} *Il23r*^{gfp/+} mice (Figure 2I). Aortic root IL23R⁺ $\gamma\delta$ T cells thus produce IL-17A and GM-CSF and HFD-feeding increases the frequency of IL-17A⁺GM-CSF⁺ IL-23R⁺ $\gamma\delta$ T cells, whereas there is a loss of IL-23R⁺ $\gamma\delta$ T cells as a source of these cytokines in *Ldlr*^{-/-} *Il23r*^{gfp/gfp} mice in the vessel wall.

3.3 Deficiency in IL-23R inhibits early atherosclerotic lesion formation

Given that IL-23R⁺ $\gamma\delta$ T cells were present in the aortic root and aorta, we assessed atherosclerotic lesion formation in *Ldlr*^{-/-} and *Ldlr*^{-/-} *Il23r*^{gfp/gfp} mice fed an HFD. IL-23R deficient *Ldlr*^{-/-} *Il23r*^{gfp/gfp} mice of both sexes showed a decrease in plaque area in the aortic root as compared to *Ldlr*^{-/-} mice after 6 weeks of HFD (Figure 3A and Supplementary material online, Figure S4a). After 12 weeks of HFD, no differences in plaque size were noted (Figure 3E). Lesion size in the aorta was unaltered at either time point (Supplementary material online, Figure S5a and b). When characterizing the plaque cell composition, no differences in the relative macrophage and SMC content were noted between *Ldlr*^{-/-} and *Ldlr*^{-/-} *Il23r*^{gfp/gfp} mice after both 6 and 12 weeks of HFD (Figure 3B, C, F and G). No differences in Ly6G⁺ neutrophils (3.2 \pm 1.1 vs. 7.8 \pm 2.8 cells/mm² plaque area in *Ldlr*^{-/-} vs. *Ldlr*^{-/-} *Il23r*^{gfp/gfp} mice, non-significant) were evidenced. No change in the relative numbers of $\alpha\beta$ ⁺ T cells but a significant decrease in $\gamma\delta$ T cells were detected in the aortic root (Supplementary material online, Figure S5c). No changes in the mRNA expression of the Th1-inducing transcription factor *Txb21*, the Th17-associated transcription factor *Rorc*, and of *Foxp3* were noted in the aortic root of *Ldlr*^{-/-} *Il23r*^{gfp/gfp} compared to *Ldlr*^{-/-} mice (Supplementary material online, Figure S5d). Notably, necrotic core size was decreased in *Ldlr*^{-/-} *Il23r*^{gfp/gfp} compared to *Ldlr*^{-/-} mice after 6 and 12 weeks of HFD (Figure 3D and H). However, no significant changes in TUNEL⁺ apoptotic cells could be evidenced (Supplementary material online, Figure S5e). Likewise, the ratio of free vs. macrophage-associated TUNEL⁺ cells, indicative of the rate of efferocytosis, was unaltered between the groups (Supplementary material online, Figure S5f). No differences in body weight or plasma cholesterol levels were noted at either time point (Table 1). These results suggest that IL-23R promotes early lesion formation in the aortic root and regulates necrotic core size.

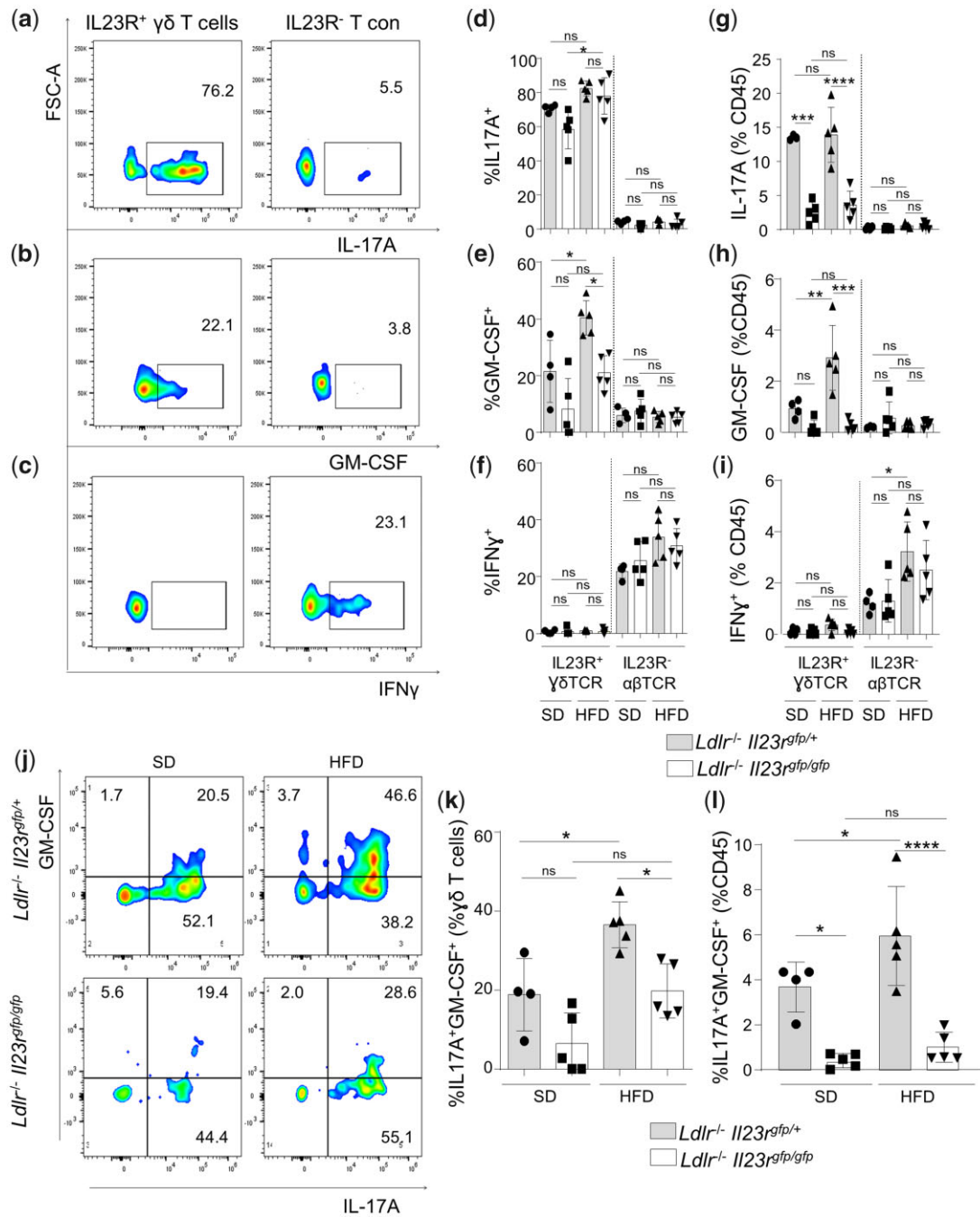


Figure 2 IL-23R⁺ $\gamma\delta$ T cells produce IL-17A and GM-CSF. (A–L) Aortic roots from *Ldlr*^{-/-} *Il23r*^{gfp/+} and *Ldlr*^{-/-} *Il23r*^{gfp/gfp} fed a SD or HFD ($n = 3–5$ mice in both groups) were analysed by flow cytometry. Representative plots of cytokine expression in IL-23R⁺ $\gamma\delta$ T cells and IL-23R⁻ $\alpha\beta$ T cells in SD-fed *Ldlr*^{-/-} *Il23r*^{gfp/+} mice (A–C). Percentages of IL17A⁺, GM-CSF⁺, and IFN γ ⁺ cells among IL-23R⁺ $\gamma\delta$ T cells and IL-23R⁻ $\alpha\beta$ T cells (D–F), and of IL17A⁺, GM-CSF⁺, and IFN γ ⁺ IL-23R⁺ $\gamma\delta$ T cells and IL-23R⁻ $\alpha\beta$ T cells among CD45⁺ cells (G–I). Representative plots of GM-CSF⁺ IL17A⁺ IL-23R⁺ $\gamma\delta$ T cells in SD and HFD-fed *Ldlr*^{-/-} *Il23r*^{gfp/+} and *Ldlr*^{-/-} *Il23r*^{gfp/gfp} mice (J), and percentages of GM-CSF⁺ IL17A⁺ cells among IL-23R⁺ $\gamma\delta$ T cells (K) and of GM-CSF⁺ IL17A⁺ IL-23R⁺ $\gamma\delta$ T cells among CD45⁺ cells (L) are shown. Statistical significance was determined by two-way ANOVA, separately performed for $\alpha\beta$ and $\gamma\delta$ T cells. Data are presented as a mean \pm SD. * $P < 0.05$, ** $P < 0.01$, *** $P < 0.001$, **** $P < 0.0001$. ns, non-significant.

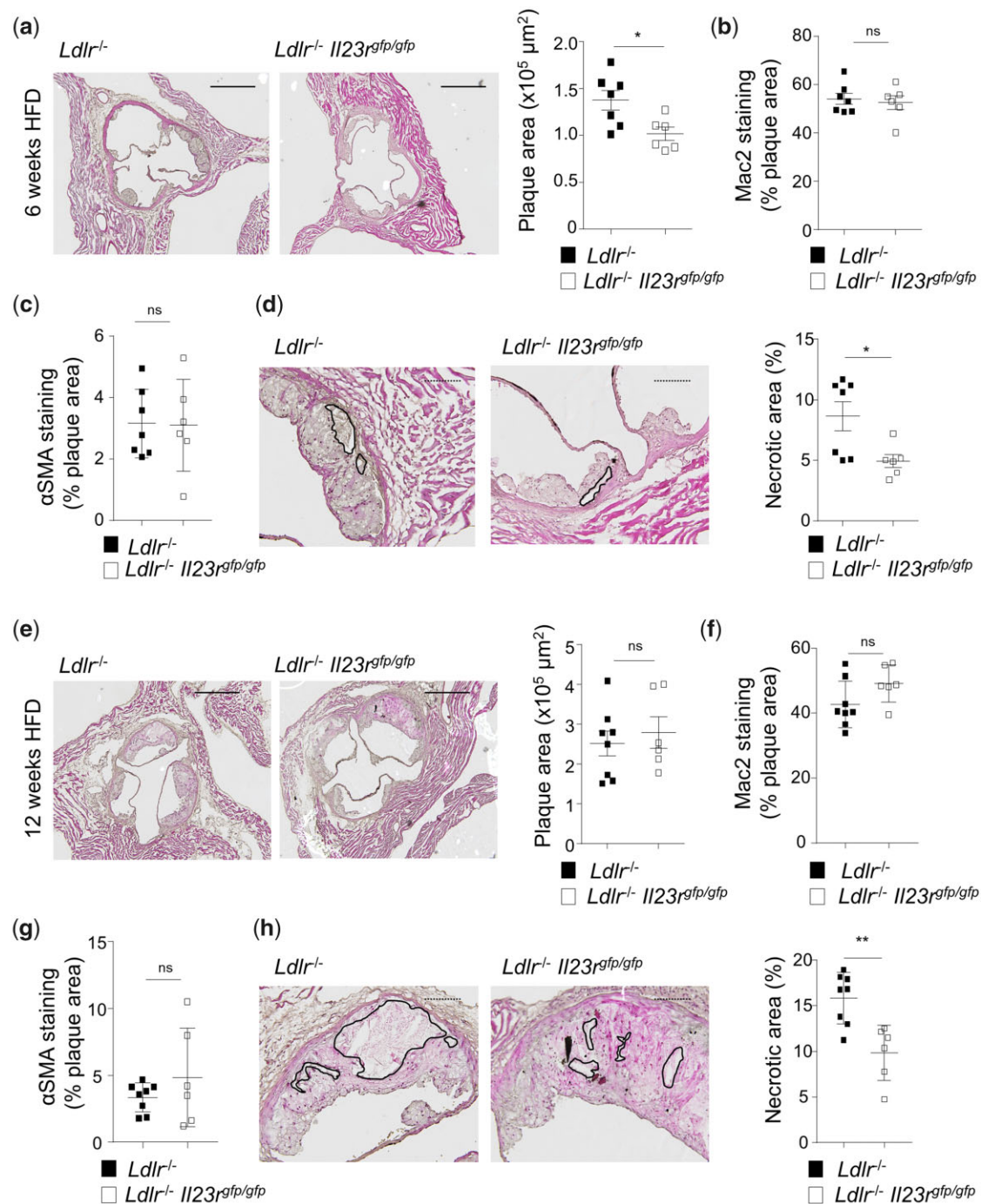


Figure 3 *Il23r* deficiency protects against early atherosclerosis in *Ldlr*^{-/-} mice in the aortic root and reduces necrotic core formation. (A–D) Male *Ldlr*^{-/-} ($n = 7$) and *Ldlr*^{-/-} *Il23r*^{gfp/gfp} mice ($n = 6$) were fed a HFD for 6 weeks, and (E–H) *Ldlr*^{-/-} ($n = 8$) and *Ldlr*^{-/-} *Il23r*^{gfp/gfp} mice ($n = 6$) were fed a HFD for 12 weeks. Representative images and quantification of plaque area in HE-stained aortic roots; Scale bars, 500 μ m (A and E). Quantification of the area positive for Mac-2 (B and F), α -smooth muscle cell actin (C and G), and of the necrotic core (D and H); representative sections with areas of necrosis circled by black traces. Quantification of necrotic areas is provided as the percent area of total lesion area. Scale bars, 100 μ m. Statistical differences were examined by unpaired Student's *t*-test. Data are presented as mean \pm SD. * $p < 0.05$, ** $p < 0.01$. ns, non-significant.

Table 1 Body weight and plasma cholesterol levels in *ldlr*^{-/-} and *ldlr*^{-/-}*Il23r*^{gfp/gfp} mice

| 6 weeks of HFD | <i>Ldlr</i> ^{-/-} (n = 7) | <i>Ldlr</i> ^{-/-} <i>Il23r</i> ^{gfp/gfp} (n = 6) | P-value |
|---------------------|------------------------------------|--------------------------------------------------------------------|---------|
| Body weight (g) | 25.6 ± 1.1 | 25.2 ± 1.6 | 0.9 |
| Cholesterol (mg/dL) | 1527 ± 114 | 1588 ± 185 | 0.7 |
| %LDL | 74.6 ± 6.4 | 80.4 ± 7.6 | 0.6 |
| %HDL | 26.6 ± 1.6 | 24.8 ± 2.3 | 0.6 |

| 12 weeks of HFD | (n = 8) | (n = 6) | P-value |
|---------------------|------------|------------|---------|
| Body weight (g) | 28.8 ± 1.8 | 28.7 ± 2.3 | 0.9 |
| Cholesterol (mg/mL) | 1718 ± 205 | 1817 ± 76 | 0.6 |

3.4 IL23R deficiency systemically alters Treg homeostasis in hypercholesterolaemic mice

Given systemic inflammatory responses in atherosclerosis, we further analysed systemic immune cell distributions in *Ldlr*^{-/-} and *ldlr*^{-/-}*Il23r*^{gfp/gfp} mice fed a HFD for 6 weeks. White blood cell counts, absolute numbers or percentages of neutrophils or monocytes did not differ between groups in the blood or spleen (Supplementary material online, Figure S6a–e). Likewise, frequencies of CD3⁺ T cells and of $\gamma\delta$ T cells were similar in the spleen and lymph nodes of *Ldlr*^{-/-} compared to *ldlr*^{-/-}*Il23r*^{gfp/gfp} mice (Supplementary material online, Figure S6f and g).

IL-23R⁺ $\gamma\delta$ T cells have been shown to restrain Treg responses during experimental autoimmune encephalomyelitis.¹⁵ In line with these findings, a small but significant increase in frequencies of CD25⁺ Foxp3⁺ CD4⁺ Tregs were noted in spleens but not peripheral lymph nodes of *ldlr*^{-/-}*Il23r*^{gfp/gfp} mice fed a HFD for 6 weeks, associated with increased splenic *Foxp3* transcript expression (Supplementary material online, Figure S7a and b). Naïve $\alpha\beta$ T cells lack IL-23R expression¹⁵ and we could not detect IL-23R on Tregs in *Il23r*^{gfp/gfp} mice (data not shown). In line, Treg frequencies did not differ after culturing isolated *Il23r*^{+/+} or *Il23r*^{gfp/gfp} naïve CD4⁺ T cells after stimulation with anti-CD3/CD28 antibodies and TGF- β upon exposure to recombinant IL-23 (Supplementary material online, Figure S7c). In total splenocytes exposed to TGF- β , however, increased percentages of Tregs were noted among *Il23r*^{gfp/gfp} compared to *Il23r*^{+/+} splenocytes (Supplementary material online, Figure S7d), suggesting indirect effects of IL-23R⁺ cells on Tregs, as previously reported.²⁹

Levels of IFN- γ ⁺-producing CD4⁺ Th1 cells were similar in lymphoid organs between *Ldlr*^{-/-} and *ldlr*^{-/-}*Il23r*^{gfp/gfp} mice and no major differences in frequencies of IL-17A-producing CD4⁺ Th17 cells were noted in both groups in mice fed a HFD for 6 weeks (Supplementary material online, Figure S6h and i), indicating that deficiency in IL23R does not entail systemic shifts in Th1 or Th17 cell frequencies.

3.5 The absence of the global pool of $\gamma\delta$ T cells does not affect atherosclerotic lesion formation

Given our findings suggesting that effects of IL-23R are $\gamma\delta$ T cell-mediated, we assessed the function of $\gamma\delta$ T cells in atherosclerotic lesion formation using δ TCR-deficient *Ldlr*^{-/-}*Tcr δ* ^{-/-} mice that lack all $\gamma\delta$ T cells. Atherosclerotic lesion size was unaltered in the aortic root after 6 weeks of HFD (Figure 4A). No differences in plaque area were observed in the aortic root after 12 weeks of HFD (Figure 4B). Blood

cholesterol levels were unchanged after 6 weeks (1258 ± 178 vs. 14 527 ± 1453 ± 259 mg/dL in *Ldlr*^{-/-} vs. *Ldlr*^{-/-}*Tcr δ* ^{-/-} mice, *P* = 0.07) or 12 weeks of diet (1014 ± 386 vs. 1083 ± 328 mg/dL in *Ldlr*^{-/-} vs. *Ldlr*^{-/-}*Tcr δ* ^{-/-} mice, *P* = 0.62). Plaque macrophage or smooth muscle cell content was not affected in the aortic root at either time point (Figure 4C and D and Supplementary material online, Figure S8a and b). However, relative necrotic core area was reduced in the aortic root of *Ldlr*^{-/-}*Tcr δ* ^{-/-} mice after 12 weeks of HFD (Figure 4E). Levels of IFN γ and IL17A-producing CD4⁺ T cells were not altered in lymph nodes and spleen (Supplementary material online, Figure S8c and d). However, an increase in the percentage of Tregs was detected in the spleen of *Ldlr*^{-/-}*Tcr δ* ^{-/-} mice after 6 weeks of HFD (Supplementary material online, Figure S8e). These data show that $\gamma\delta$ T cells restrain systemic Treg responses during atherogenesis, and promote plaque necrosis.

3.6 IL-23 is produced in the aortic root

In vitro studies demonstrated IL-23 production by activated dendritic cells and macrophages.³⁰ In scRNA-seq analyses of aortic cells, *Il23a* transcripts were poorly detected, but rare *Il23a* positive cells localized to e.g. mononuclear phagocytes and SiglecF⁺ neutrophils²⁴ (Supplementary material online, Figure S3c and d). To further investigate IL-23 production in antigen-presenting cells, BM-APCs were cultured and stimulated with different atherosclerosis-relevant stimuli. LPS but not native LDL (nLDL) or oxLDL alone induced IL-23 cytokine production in cultured cells within 24 h of stimulation (Figure 5A). In BM-APCs exposed to lipopolysaccharide (LPS), however, co-incubation of LPS with oxLDL but not nLDL further increased IL-23 production in a concentration-dependent manner (Figure 5A and B), suggesting that activation of TLR-4 triggers IL-23 expression in BM-APCs that is potentiated by additional oxLDL-mediated signalling. Of note, in *Ldlr*^{-/-} mice, an increased expression of *Il23a* mRNA was found specifically in the aortic root, but not in the aorta or spleen after 6 weeks of HFD compared to SD (Figure 5C). We also evaluated IL-23 production in tissue digests of SD and HFD-fed *Ldlr*^{-/-} mice, stimulated with LPS and oxLDL, by flow cytometry. While some intracellular IL-23 staining was seen in macrophages and dendritic cells in the aorta and spleen in both SD and HFD-fed mice, significantly increased frequencies of IL-23⁺ macrophages were detectable in the aortic root of HFD-fed vs. SD-fed *Ldlr*^{-/-} mice and compared to macrophages in the aorta (Figure 5D, Supplementary material online, Figure S9). These data clearly show that macrophages/dendritic cells serve as a source of IL-23 in the aortic root, further corroborating local functions of IL-23/IL-23R in promoting early inflammation in atherosclerosis.

3.7 Cytokines associated with IL-23R⁺ $\gamma\delta$ T cells induce macrophage necroptosis

IL-23 signalling, induced by GM-CSF, has previously been associated with the induction of macrophage apoptosis and plaque necrosis in *Ldlr*^{-/-}*Csf2*^{-/-} mice.¹⁸ By scRNA-seq, we could not detect *Il23r* transcripts in *Csf1r*⁺*Adgre1*⁺ macrophages and other aortic CD45⁺ cell populations (Figure 1C and D and Supplementary material online, Figure S3a and b). Similarly, cytometric analyses of the aortic root and aorta revealed no IL-23R expression in myeloid cells, including CD11c⁺F4/80⁺ or CD11c⁺MHCII⁺ APCs, or CD19⁺ B cells of *Ldlr*^{-/-}*Il23r*^{gfp/gfp} mice (Supplementary material online, Figure S10, and data not shown). As IL-23R deficiency reduces necrotic core size in *Ldlr*^{-/-} mice, we assessed whether the cytokines released from IL23R⁺ $\gamma\delta$ T cells could directly affect macrophage cell death. Treatment of BMDMs

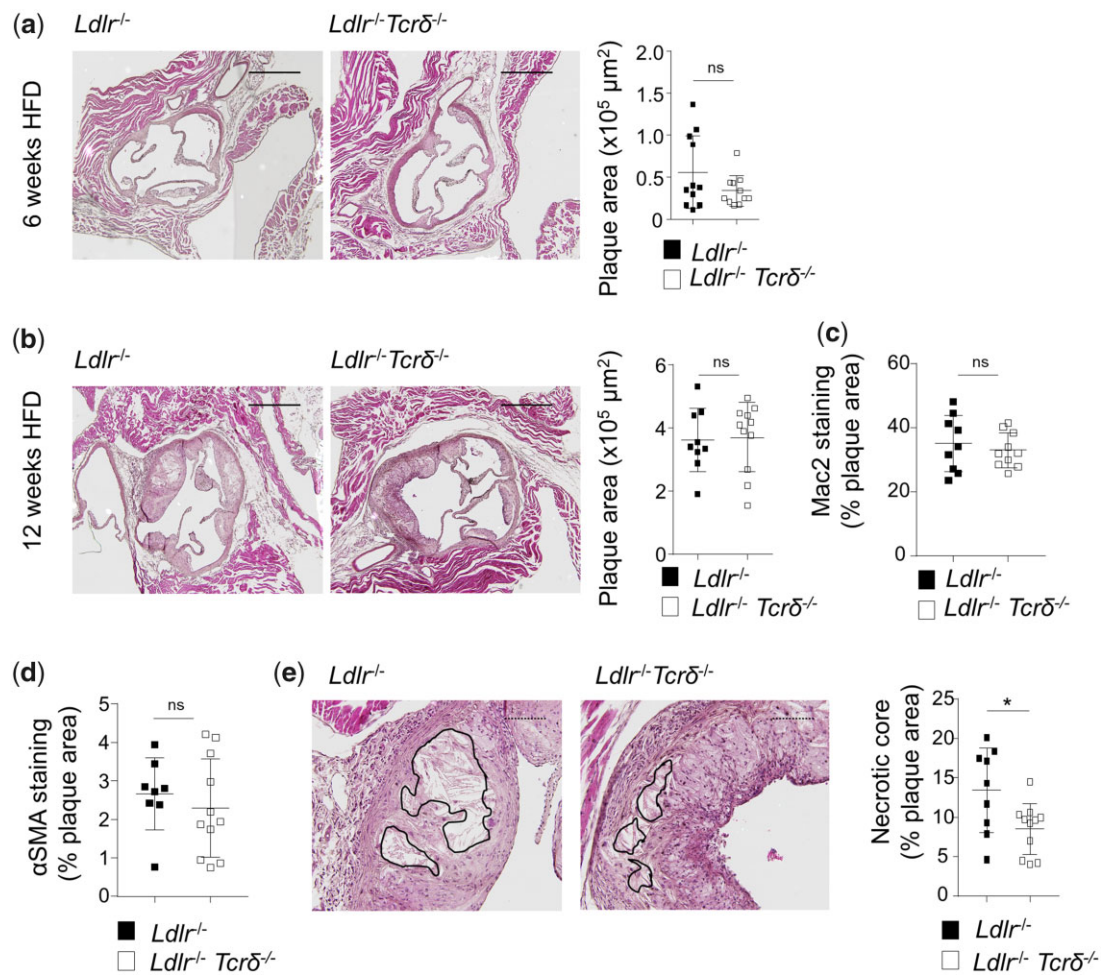


Figure 4 Lack of $\gamma\delta$ T cells in *Ldlr*^{-/-} mice does not alter plaque size but reduces necrotic core formation. (A) *Ldlr*^{-/-} ($n = 11$) and *Ldlr*^{-/-}*Tcrδ*^{-/-} mice ($n = 11$) were fed a HFD for 6 weeks, and (B–E) *Ldlr*^{-/-} ($n = 8–9$) and *Ldlr*^{-/-}*Tcrδ*^{-/-} mice ($n = 10–11$) were fed a HFD for 12 weeks. Representative images and quantification of plaque area in HE-stained aortic roots, scale bars, 500 μm (A and B). Quantification of the area positive for Mac-2 (C), α -smooth muscle cell actin (D), and of the necrotic core scale bars (E); Representative sections with areas of necrosis circled by black traces. Quantification of necrotic areas is provided as the percent area of total lesion area. Scale bars, 100 μm . Statistical differences were examined by unpaired Student's *t*-test. Data are presented as mean \pm SD. * $P < 0.05$. ns, non-significant.

with IL-17A, GM-CSF, or both cytokines alone did not modulate the rate of apoptosis. In contrast, frequencies of necrotic BMDMs increased upon treatment with GM-CSF but in particular when exposed to both GM-CSF and IL-17A (Figure 6A). We further evaluated expression of key signalling molecules regulating apoptosis and necroptosis.³¹ Expression of apoptosis-associated total Caspase 3 and Caspase 8 did not change, and no cleavage of Caspase 3 or Caspase 8 was detectable (Supplementary material online, Figure S11). Cell death via the necroptotic pathway is induced by activation of the protein kinases RIPK3 and RIPK1, and the pursuant RIPK3-mediated phosphorylation of mixed lineage kinase domain-like (MLKL).³¹ mRNA expression of *Ripk3* and *Mkl1* but not *Ripk1* were increased in BMDMs treated with IL-17A and GM-CSF as compared to untreated BMDMs (Figure 6B), and increased RIPK1, RIPK3, and MLKL protein levels were noted in IL-17A and GM-CSF-treated BMDMs (Figure 6C), suggesting the induction of necroptosis. Necroptosis can function as a trigger of inflammation.³¹ Treatment of BM-APCs with IL17A and GM-CSF induced inflammatory iNOS-

encoding gene *Nos2*, and inflammatory *Tnfa*, *Il6*, *Nlrp3*, *Il1b*, and *Ccl2*, whereas anti-inflammatory *Il10* transcripts were reduced and *Il18* expression was unaltered (Figure 6D). Accordingly, decreased *lfn3* and increased *Il10* mRNA expression was noted in atherosclerotic aortic roots of *Ldlr*^{-/-}*Il23*^{gfp/gfp} compared to *Ldlr*^{-/-} mice (Figure 6E). This could imply that IL-23R signalling in $\gamma\delta$ T cells, via the production of IL-17A and GM-CSF, increases plaque necrosis and inflammation in the aortic root in atherosclerosis.

4. Discussion

IL-23R expression has previously been shown to characterize pathogenic Th17 cells,⁹ and to be expressed by $\gamma\delta$ T cells that respond to IL-23 with the secretion of cytokines and the ability to antagonize Treg functions.¹⁵ $\gamma\delta$ T cells, however, have been reported to have no major function in experimental atherosclerosis.^{7,8} We, here demonstrate that IL-23R expression was mostly confined to $\gamma\delta$ T cells in the aortic root

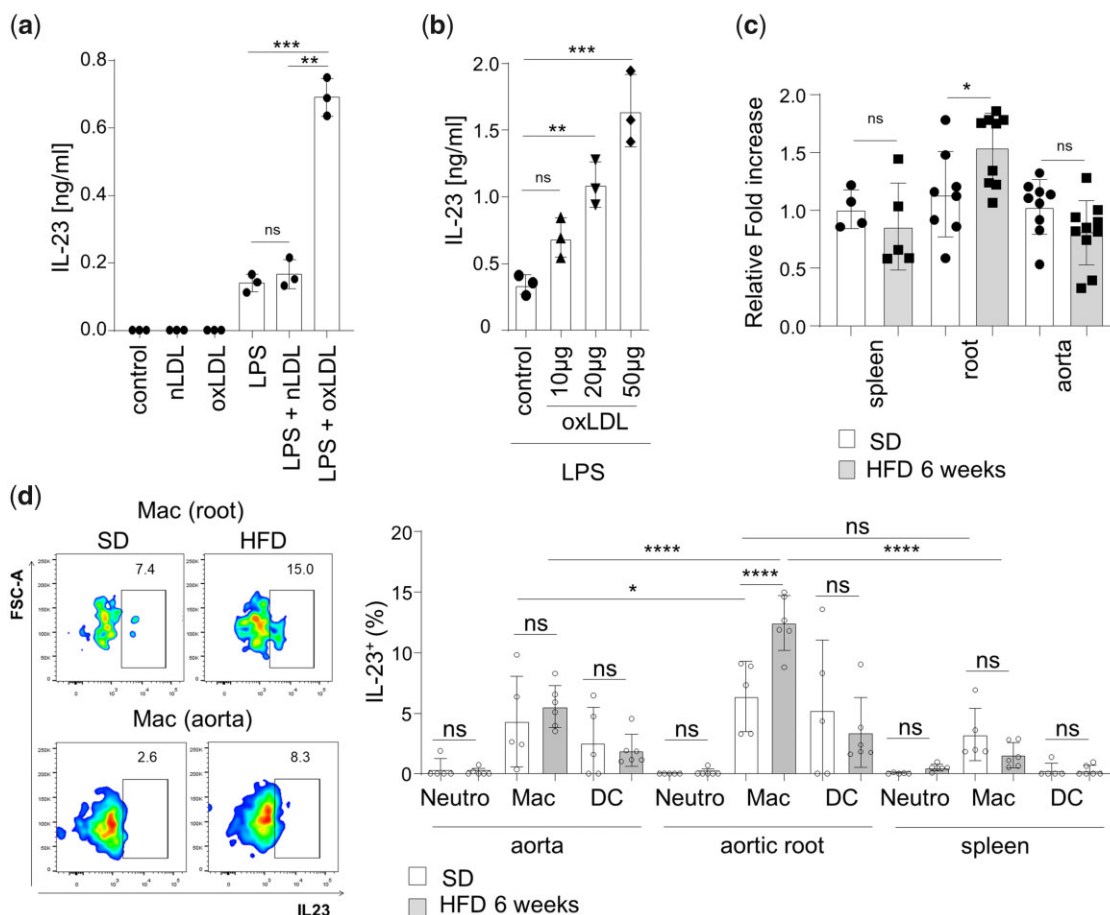


Figure 5 oxLDL amplifies IL-23 secretion by BM-APCs. (A and B) BM-APCs were left untreated, or (co-) incubated with nLDL (50 $\mu\text{g}/\text{mL}$), oxLDL (50 $\mu\text{g}/\text{mL}$), or LPS (100 ng/mL), or (co-) incubated with LPS (100 ng/mL) and oxLDL (indicated concentrations) (B) overnight. Levels of IL-23 were measured from cell-free supernatants by ELISA. One out of three independent experiments performed with $n = 3$ BM-APC cultures from three distinct mice per experiment. (C) *Il23a* mRNA expression in the spleen, root or aorta of *Ldlr*^{-/-} mice fed a SD (spleen $n = 4$, root $n = 8$, and aorta $n = 9$) or a HFD for 6 weeks (spleen $n = 5$, root $n = 9$, and aorta $n = 10$). Results were normalized to *Hprt* and presented relative to *Ldlr*^{-/-} mice fed a SD. Statistical differences were examined by unpaired Student's *t*-test. (D) Aortas, aortic roots, and spleens from *Ldlr*^{-/-} mice fed a SD ($n = 5$) or HFD ($n = 6$ mice) were analysed by flow cytometry. Representative plots of macrophages from the root and aorta of SD and HFD-fed *Ldlr*^{-/-} mice. Percentages of IL-23R⁺ cells among CD11b⁺Ly6G⁺ neutrophils, CD11b⁺F4/80⁺ macrophages, and CD11b⁺CD11c⁺MHCII⁺ dendritic cells. Statistical significance was determined by two-way ANOVA, separately performed for neutrophils, macrophages, and dendritic cells. Data are presented as mean \pm SD. * $P < 0.05$, ** $P < 0.01$. *** $P < 0.001$. ns, non-significant.

and aorta. Whereas IL-23R⁺ $\gamma\delta$ T cells were frequent in the aortic root, fewer cells were identified in the aorta. Mice overexpressing IL-23 have been shown to develop inflammation in the aortic sinus, and flow cytometric analyses demonstrated the presence of IL-23R⁺ CD3⁺CD4⁺CD8⁻ T cells at this site.²¹ These were likely $\gamma\delta$ T cells, as more recently suggested by immunofluorescence staining in *Tcrd-H2BeGFP* reporter mice.⁶ Similarly, we could observe IL-23R⁺ cells in the aortic root of *Ldlr*^{-/-}*Il23r*^{gfp/+} mice by two-photon microscopy. It was suggested that these $\gamma\delta$ T cells constitute a cell population similar to foetal thymus-dependent resident enthesal V γ 6⁺IL-23R⁺IL-17⁺ $\gamma\delta$ T cells that can be found specifically at sites of high biomechanical stress and trigger enthesitis in mice.⁶ The cell population of aortic root $\gamma\delta$ T cells may indeed comprise this V γ 6⁺ subset, as suggested by PCR profiling (unpublished observations). Aortic valves share histological similarities with peripheral entheses, including the presence of cartilage and chondrocytes where

the valve joins the aorta and where the valve moves and flexes like entheses.²¹ In entheses, $\gamma\delta$ T cells have been shown to be tethered and not motile, as opposed to lymph node or dermal $\gamma\delta$ T cells.⁶ Also in parabiotic mice, dermal and lymph node-derived IL-17-producing V γ 6⁺ $\gamma\delta$ T cells were principally, but not exclusively, shown to be tissue-resident, suggesting that V γ 6⁺ T cells locally adapt to specific sites of the body as resident cells while possibly retaining the capability to circulate between tissues.³² This may suggest that $\gamma\delta$ T cells are a mostly tissue-resident cell population in the aortic root. Given the accumulation of $\gamma\delta$ T cells in joint enthesal regions and the aortic valve and root, Reinhardt *et al.*⁶ proposed that the accumulation of $\gamma\delta$ T cells in different enthesal-related tissues reveals a common IL-23-driven mechanism. Indeed, the presence of $\gamma\delta$ T cells in the vasculature was IL-23R-dependent, as a marked reduction in aortic root $\gamma\delta$ T cells was noted in mice deficient in IL-23R. The exact $\gamma\delta$ T-cell subset in the aortic root vs. the aorta or

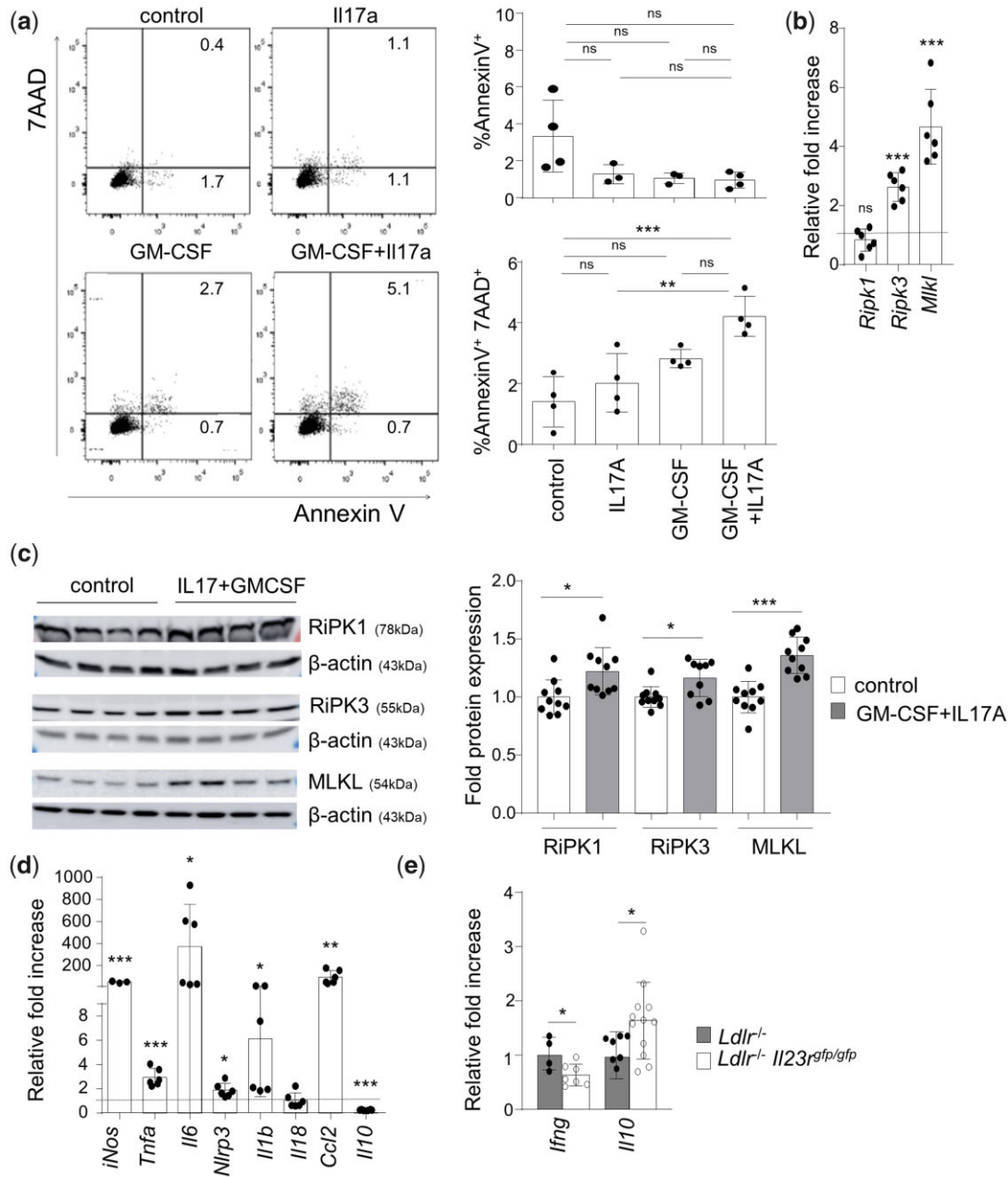


Figure 6 Cytokines associated with IL-23R⁺ γδT cells induce macrophage necroptosis. (A–D) BMDMs were stimulated with GM-CSF (25 ng/mL) and/or rIL17A (25 ng/mL) for 24 h. (A) AnnexinV and 7AAD staining was analysed by flow cytometry. Representative plots from two independent experiments, each performed with *n* = 3–4 BMDM cultures from distinct mice, and percentages of AnnexinV⁺ apoptotic and AnnexinV⁺ 7AAD⁺ necrotic cells among CD45⁺ CD11b⁺ F4/80⁺ macrophages. Statistical differences were examined by one-way ANOVA (B) *Ripk1*, *Ripk3*, and *Mlkl* mRNA expression, as analysed by qPCR (*n* = 6 mice). (C) Protein expression was analysed by Western Blotting. Representative blot from three independent experiments performed with *n* = 3–4 mice per experiment, and quantification of protein expression relative to β-actin and control-treated cells (*n* = 9–10 mice). (D) mRNA expression of indicated genes was analysed by qPCR; results were normalized to *Hprt* and presented relative to untreated controls (*n* = 3–6 mice). (E) mRNA expression of *Ifng* and *Il10* in the aortic root of *Ldlr*^{-/-} (*n* = 4–7) and *Ldlr*^{-/-} *Il23rgfp/gfp* mice (*n* = 7–12) fed a HFD for 6 weeks; results were normalized to *Hprt* and presented relative to *Ldlr*^{-/-} controls (E). Statistical differences were examined by unpaired Student's *t*-test. Data are presented as mean ± SD. **P* < 0.05, ***P* < 0.01, ****P* < 0.001. ns, non-significant.

lymphoid organs, and whether IL-23R has role in the embryonic recruitment or local maintenance of γδ T cells, however, remains to be established.

In enthesal organs permanently exposed to mechanical forces, microdamage may activate enthesal-resident γδ T cells to trigger the

production of proinflammatory cytokines, such as IL-17A.^{6,21} The role of IL-23R⁺ γδ T cells in the vasculature under homeostatic conditions is unclear. Previous reports demonstrated that IL-23 is important for the clearance of extracellular pathogens,³³ suggesting a role in homeostatic tissue defence. We here addressed the role of IL-23R and γδ T cells in

atherosclerotic lesion formation. When fed a HFD for 6 weeks, IL-23R-deficiency reduced the size of early atherosclerotic lesions in the aortic root. In contrast, mice deficient in $\gamma\delta$ T cells did not show differences in atherosclerotic lesion size. These findings suggest an atherogenic role of IL-23R⁺ $\gamma\delta$ T cells in early lesion formation in the aortic root. The loss of this atherogenic $\gamma\delta$ T-cell subset but also of potentially non-pathogenic IL23R⁻ $\gamma\delta$ T cells may have resulted in a net unaltered plaque size in the aortic root in *Ldlr*^{-/-}*Tcr δ* ^{-/-} mice. At more advanced stages of lesion formation, after 12 weeks of HFD, no effects on lesion size were noted in either *Ldlr*^{-/-}*Il23r*^{gfp/gfp} or *Ldlr*^{-/-}*Tcr δ* ^{-/-} mice. This is in line with previous findings showing unaltered atherosclerotic lesion size in *Ldlr*^{-/-}*Il23r*^{gfp/gfp} mice after 10 weeks of HFD feeding,¹⁹ and in *Apoe*^{-/-}*Tcr δ* ^{-/-} mice with mild hypercholesterolaemia (mice fed a SD for 18 weeks)⁸ or after 10 weeks of HFD-feeding.⁷ At later stages of lesion formation, however, IL-23 has been shown to protect from diet-induced atherosclerosis in *Ldlr*^{-/-} mice by maintaining the intestinal barrier and preventing pro-atherogenic bacteria expansion and metabolite production.²⁰ The at least partial loss of such systemic protective effects of IL-23 responses in the gut in *Ldlr*^{-/-}*Il23r*^{gfp/gfp} mice may have attenuated local atheroprotective effects derived from the loss of pathogenic IL-23R signalling in the aortic root also at earlier lesion stages, and contributed to the rather mild atherosclerosis phenotype.

Mice deficient in IL-23R as well as mice lacking $\gamma\delta$ T cells developed plaques characterized by reduced relative necrotic core area, after both 6 and 12 weeks of HFD. IL-23R-deficient mice in addition showed reduced aortic inflammation, as suggested by increased expression of IL-10 but decreased levels of IFN- γ . GM-CSF has previously been shown to induce IL-23 in myeloid cells, which in turn increases apoptosis susceptibility of macrophages. Accordingly, GM-CSF-deficient *Ldlr*^{-/-} mice displayed reduced lesional necrotic core area and a decrease in IL-23 and IFN- γ expression.¹⁸ It may thus be conceivable that IL-23R⁺ $\gamma\delta$ T-cell activation associated with GM-CSF secretion propagated local IL-23 production, in turn inducing macrophage apoptosis, and plaque necrosis and inflammation.¹⁸ It should be noted, however, that we could not detect IL-23R expression on vascular macrophages *in vivo* or in BMDMs *in vitro*, so that it remains to be elucidated whether IL-23 can directly affect macrophage cell death. We here observed that GM-CSF alone can trigger a mild increase in BMDM cell death, but exposure of BMDMs to GM-CSF together with IL-17 markedly increased BMDM necrosis but not apoptosis *in vitro*, and induced signalling pathways associated with necroptosis, including the expression of RIPK1, RIPK3, and MLKL. RIPK1 activates RIPK3, which subsequently phosphorylates MLKL to induce necroptosis.³⁴ Interestingly, RIPK1 is expressed in early-stage atherosclerotic lesions in humans and mice and drives atherosclerosis and inflammation by its ability to activate NF- κ B and inflammatory cytokine production in diet-fed *Apoe*^{-/-} mice.³⁵ RIPK3-mediated necroptosis was demonstrated to play a crucial role in necrotic core formation and atherosclerosis.³⁶ Also, MLKL contributes to necrotic core formation in atherosclerosis.³⁷ Activation of RIPK1, RPK3, and MLKL by IL-17/GM-CSF may thus have contributed to IL-23R-induced necrotic core formation and inflammation in our study. Of note, MLKL also has anti-atherogenic functions by limiting lipid accumulation in foam cells within plaques.³⁷ Increased MLKL expression in BMDMs exposed to IL-17/GM-CSF may thus promote their necroptotic cell death but also reduce foam cell formation independent of cell death, and both mechanisms may have contributed during early lesion formation in *Ldlr*^{-/-}*Il23r*^{gfp/gfp} mice. In addition, direct and cytotoxic effects of $\gamma\delta$ T cells on macrophages may be conceivable, as activated $\gamma\delta$ T cells can acquire cytotoxic activity to eliminate macrophages.^{38,39}

We here show that IL-23R⁺ $\gamma\delta$ T cells have a strong propensity towards IL-17 production, and scRNA-seq analyses corroborated that IL23R⁺ $\gamma\delta$ T cells were the main source of IL-17 production in the aorta in atherosclerotic *Ldlr*^{-/-} mice. In the few IL-23R⁺ $\gamma\delta$ T cells that remained in the *Ldlr*^{-/-}*Il23r*^{gfp/gfp} mice, we did not observe a reduction in IL-17A secretion in SD and HFD-fed mice compared to *Ldlr*^{-/-}*Il23r*^{gfp/+} mice, which may suggest alternative pathways that control IL-17A production in these cells in the absence of IL-23R signalling. Some IL23R⁺ $\gamma\delta$ T cells also produced GM-CSF, which increased upon HFD feeding, and single $\gamma\delta$ T cells expressing this cytokine were also found by scRNA-seq, although GM-CSF expression predominated in ILC2s. GM-CSF production by other cell type, such as ILC2s may thus have complemented IL-17 secretion from IL-23R⁺ $\gamma\delta$ T cells to induce necroptosis and inflammation in atherosclerosis, in addition to the pathogenic IL-17⁺GM-CSF⁺IL23R⁺ $\gamma\delta$ T cells. Notably, IL-23 together with IL-1 β expression is indispensable for GM-CSF expression by central nervous system-infiltrating T cells,⁴⁰ and the combination of IL-23 together with IL-1 β is required for GM-CSF production by $\gamma\delta$ T cells in the absence of TCR stimulation in experimental autoimmune encephalomyelitis.¹⁷ The cytokine IL-1 β is induced early in macrophages in diet-induced atherosclerosis.⁴¹ Both IL-1 β and IL-23, together with other mediators induced by HFD-feeding, may thus have contributed to GM-CSF production by $\gamma\delta$ T cells in atherosclerosis.

We did not observe aortic CD4⁺ T cells a major source of IL-17 in our study. In a prior study investigating diet-fed *Ldlr*^{-/-}*Il23r*^{gfp/gfp} mice, pathogenic Th17 cells comprised a small population of cells (0.05% of CD4⁺ T-helper cells) in lymphoid organs, which was unaffected by deficiency of IL-23 and undetectable in the aorta. Moreover, the transfer of CD4⁺ T-helper cells from *Ldlr*^{-/-}*Il23r*^{gfp/gfp} mice into *Ldlr*^{-/-}*Rag1*^{-/-} mice did not entail a reduction in lesion formation or change in plaque phenotype,¹⁹ furthermore supporting the notion that IL-23R⁺CD4⁺ Th17 cells do not contribute substantially to the phenotype observed in *Ldlr*^{-/-}*Il23r*^{gfp/gfp} mice in early atherosclerosis.

We also found that IL-23R deficiency was accompanied by a mild increase in frequencies of Tregs in spleens but not lymph nodes of HFD-fed mice, in line with previous observations in *Il23r*^{gfp/gfp} mice.^{29,42,43} We did not detect significant changes in *Foxp3* mRNA expression in the aortic root, but *Il10* cytokine expression was elevated at this site. Given the atheroprotective effects of this cell subset⁴⁴ and the low abundance of Tregs in the vasculature,⁴⁵ differences in few cells may have gone unnoticed by evaluating mRNA expression, and Tregs may have contributed to local atheroprotective effects in *Ldlr*^{-/-}*Il23r*^{gfp/gfp} mice. However, increased frequencies of splenic Tregs were similarly observed in diet-fed *Ldlr*^{-/-}*Tcr δ* ^{-/-} mice without alterations in atherosclerotic lesion formation, arguing against a major role of these mild systemic changes in Tregs on early atherosclerotic lesion formation in our study.

Interestingly, we noted increased *Il23a* expression in the aortic root but not aorta upon HFD-feeding, which could be in line with a local $\gamma\delta$ T-cell response. *In vitro*, oxLDL potentiated and sustained the release of IL-23 from LPS-activated BM-APCs. Increased levels of *Il23a* in the aortic root could also be in line with the previously documented predominant localization of APCs in the aortic valve and sinus compared to the aorta.⁴⁶ In atherosclerosis, TLR activation by oxLDL or low grade endotoxemia^{47,48} in addition to uptake of oxLDL may thus trigger IL-23 production by APCs to activate atherogenic IL-23R⁺ $\gamma\delta$ T cells in the aortic sinus. GM-CSF secretion by $\gamma\delta$ T cells may then further amplify IL-23 production in APCs¹⁸ in a positive feed-forward mechanism. Another source of IL-23 are neutrophils.⁴⁹ Neutrophils, regarded as the first line of defence against infection, are more abundant in early atherosclerotic

lesions compared to more advanced plaques⁵⁰ and via IL-23 secretion could work together with IL-23R⁺ $\gamma\delta$ T cells to instigate inflammation in the vessel wall. After stimulation of vascular tissue digests or splenocytes with LPS/oxLDL *ex vivo*, however, we could not detect intracellular IL-23 in neutrophils, but this may relate to suboptimal stimulation conditions for this cell type. IL-23 production was mostly confined to macrophages and some dendritic cells in this setting. Reporter mouse models will be useful to *in vivo* trace cellular and temporal IL-23 expression patterns in atherosclerosis in the future.

In past years, several studies have associated IL-23 with cardiovascular diseases, such as peripheral artery disease⁵¹ and carotid atherosclerosis.⁵² Based on our findings one may speculate that IL-23 affects local plaque formation and plaque necrosis. Given that large necrotic cores are a hallmark of vulnerable plaques,⁵³ IL-23 may contribute to plaque instability and in consequence adverse cardiovascular events. Different clinical trials using antibodies against p19 (unique to IL-23) are currently being tested for the treatment of psoriasis. It will be interesting to monitor whether p19 blockade reduces the increased risk of cardiovascular events in these patients. Interestingly, p19 subunits are abundant in Giant-cell arteritis,⁵⁴ and targeting IL-12/IL-23 was shown to be effective for the treatment of this disease.⁵⁵ Given the location of IL-23R⁺ $\gamma\delta$ T cells in the vessel wall, our findings could also be relevant to this pathology.

In summary, we demonstrate that IL-23R⁺ $\gamma\delta$ T cells are present in the aortic root and express IL-17 and GM-CSF. IL-23R⁺ $\gamma\delta$ T cells play an important role in locally promoting lesion formation, plaque necrosis and inflammation in the aortic root. Targeting the IL-23/IL-23R-axis could thus be further explored as a therapeutic option for the inhibition of early atherosclerotic lesion formation.

Supplementary material

Supplementary material is available at *Cardiovascular Research* online.

Authors' contributions

J.G.-P., N.A., I.J., H.D.M., A.B., A.-E.S., K.L., L.B., I.P., A.W., T.K., C.C., and A.Z. designed the project and experiments; J.G.-P., N.A., I.J., H.D.M., M.R., T.B., P.C., S.S., and C.C. performed the experiments and analysed the results. J.G.-P. and A.Z. drafted the original manuscript. All authors provided critical input, critically reviewed the article, and contributed to discussion and interpretation of results.

Acknowledgements

We thank Petra Hönig-Liedl for expert technical assistance, and Nina DiFabion, Tobias Krammer, and Panagiota Arampatzis for technical assistance with single-cell RNA-seq library preparation, sequencing, and pre-processing. Illustrations of cell types in the graphical abstract are based on graphics from Servier Medical Art.

Conflict of interest: none declared.

Funding

This project was supported by the Deutsche Forschungsgemeinschaft (374031971—TRR 240, 324392634—TR221, ZE827/13-1, 14-1, 15-1, and 16-1 to A.Z.; PR727/11-2 and 13-1 to I.P.; 236177352- SFB 1116, TPA09 to

K.L.; TRR156, CRC1292 and Reinhart Koselleck grant to A.W.; TRR128, TRR274, SFB1054, and the Synergy excellence cluster EXC 2145, ID 390857198 to T.K.; CO1220/1-1 and CO1220/3-1 to C.C.), the Interdisciplinary Center for Clinical Research (IZKF), University Hospital Würzburg (E-352 and A-384 to A.Z., and E-353 to C.C.), the BMBF within the Comprehensive Heart Failure Centre Würzburg (BMBF 01EO1504 to C.C.). T.K. receives funding from the ERC (CoG 647215).

Data availability

Single-cell RNA sequencing data are accessible in Gene Expression Omnibus under the accession number GSE182950 (Figure 1) and GSE97310 (previously published data from Cochain et al. *Circ Res* 2018). Other raw data underlying this article are available upon request.

References

- Cochain C, Zerneck A. Macrophages in vascular inflammation and atherosclerosis. *Pflugers Arch* 2017;**469**:485–499.
- Tabas I. 2016 Russell Ross Memorial Lecture in Vascular Biology: molecular-cellular mechanisms in the progression of atherosclerosis. *Arterioscler Thromb Vasc Biol* 2017;**37**:183–189.
- Leeper NJ. The role of necroptosis in atherosclerotic disease. *JACC Basic Transl Sci* 2016;**1**:548–550.
- Ait-Oufella H, Sage AP, Mallat Z, Tedgui A. Adaptive (T and B cells) immunity and control by dendritic cells in atherosclerosis. *Circ Res* 2014;**114**:1640–1660.
- Kleindienst R, Xu Q, Willeit J, Waldenberger FR, Weimann S, Wick G. Immunology of atherosclerosis. Demonstration of heat shock protein 60 expression and T lymphocytes bearing alpha/beta or gamma/delta receptor in human atherosclerotic lesions. *Am J Pathol* 1993;**142**:1927–1937.
- Reinhardt A, Yevsy T, Worbs T, Lienenklaus S, Sandrock I, Oberdorfer L, Korn T, Weiss S, Forster R, Prinz I. Interleukin-23-dependent gamma/delta T cells produce interleukin-17 and accumulate in the entheses, aortic valve, and ciliary body in mice. *Arthritis Rheumatol* 2016;**68**:2476–2486.
- Cheng HY, Wu R, Hedrick CC. Gammadelta (gammadelta) T lymphocytes do not impact the development of early atherosclerosis. *Atherosclerosis* 2014;**234**:265–269.
- Elhage R, Gourdy P, Brouchet L, Jawien J, Fouque MJ, Fievet C, Huc X, Barreira Y, Couloumiers JC, Arnal JF, Bayard F. Deleting TCR alpha beta+ or CD4+ T lymphocytes leads to opposite effects on site-specific atherosclerosis in female apolipoprotein E-deficient mice. *Am J Pathol* 2004;**165**:2013–2018.
- Awasthi A, Riolo-Blanco L, Jager A, Korn T, Pot C, Galileos G, Bettelli E, Kuchroo VK, Oukka M. Cutting edge: IL-23 receptor gfp reporter mice reveal distinct populations of IL-17-producing cells. *J Immunol* 2009;**182**:5904–5908.
- Vignali DA, Kuchroo VK. IL-12 family cytokines: immunological playmakers. *Nat Immunol* 2012;**13**:722–728.
- Burkett PR, Meyer zu Horste G, Kuchroo VK. Pouring fuel on the fire: th17 cells, the environment, and autoimmunity. *J Clin Invest* 2015;**125**:2211–2219.
- El-Behi M, Ciric B, Dai H, Yan Y, Cullimore M, Safavi F, Zhang GX, Dittel BN, Rostami A. The encephalitogenicity of T(H)17 cells is dependent on IL-1- and IL-23-induced production of the cytokine GM-CSF. *Nat Immunol* 2011;**12**:568–575.
- Gaffen SL, Jain R, Garg AV, Cua DJ. The IL-23-IL-17 immune axis: from mechanisms to therapeutic testing. *Nat Rev Immunol* 2014;**14**:585–600.
- Taleb S, Tedgui A. IL-17 in atherosclerosis: the good and the bad. *Cardiovasc Res* 2018;**114**:7–9.
- Petermann F, Rothhammer V, Claussen MC, Haas JD, Blanco LR, Heink S, Prinz I, Hemmer B, Kuchroo VK, Oukka M, Korn T. gammadelta T cells enhance autoimmunity by restraining regulatory T cell responses via an interleukin-23-dependent mechanism. *Immunity* 2010;**33**:351–363.
- Sutton CE, Lalor SJ, Sweeney CM, Brereton CF, Lavelle EC, Mills KH. Interleukin-1 and IL-23 induce innate IL-17 production from gammadelta T cells, amplifying Th17 responses and autoimmunity. *Immunity* 2009;**31**:331–341.
- Lukens JR, Barr MJ, Chaplin DD, Chi H, Kanneganti TD. Inflammasome-derived IL-1beta regulates the production of GM-CSF by CD4(+) T cells and gammadelta T cells. *J Immunol* 2012;**188**:3107–3115.
- Subramanian M, Thorp E, Tabas I. Identification of a non-growth factor role for GM-CSF in advanced atherosclerosis: promotion of macrophage apoptosis and plaque necrosis through IL-23 signaling. *Circ Res* 2015;**116**:e13–e24.
- Engelbertsen D, Depuydt MAC, Verwilligen RAF, Rattik S, Levinsohn E, Edsfeldt A, Kuperwaser F, Jarolim P, Lichtman AH. IL-23R deficiency does not impact atherosclerotic plaque development in mice. *J Am Heart Assoc* 2018;**7**:e008257.
- Fatkhullina AR, Peshkova IO, Dzusev A, Aghayev T, McCulloch JA, Thovarai V, Badger JH, Vats R, Sundt P, Tang HY, Kossenkov AV, Hazen SL, Trinchieri G, Griwnnikov SI, Koltsova EK. An interleukin-23-interleukin-22 axis regulates intestinal

- microbial homeostasis to protect from diet-induced atherosclerosis. *Immunity* 2018; **49**:943–957.e9.
21. Sherlock JP, Joyce-Shaikh B, Turner SP, Chao CC, Sathe M, Grein J, Gorman DM, Bowman EP, McClanahan TK, Yearley JH, Eberl G, Buckley CD, Kastelein RA, Pierce RH, Laface DM, Cua DJ. IL-23 induces spondyloarthritis by acting on ROR-gammat+ CD3+CD4-CD8- enthesal resident T cells. *Nat Med* 2012; **18**:1069–1076.
 22. Bonneville M, O'Brien RL, Born WK. Gammadelta T cell effector functions: a blend of innate programming and acquired plasticity. *Nat Rev Immunol* 2010; **10**:467–478.
 23. Papotto PH, Reinhardt A, Prinz I, Silva-Santos B. Innately versatile: gammadelta17 T cells in inflammatory and autoimmune diseases. *J Autoimmun* 2018; **87**:26–37.
 24. Vafadarnejad E, Rizzo G, Krampert L, Arampatzi P, Arias-Loza AP, Nazzari Y, Rizakou A, Knochenhauer T, Bandi SR, Nugroho VA, Schulz DJ, Roesch M, Alayrac P, Vilar J, Silvestre JS, Zerneck A, Saliba AE, Cochain C. Dynamics of cardiac neutrophil diversity in murine myocardial infarction. *Circ Res* 2020; **127**:e232–e249.
 25. Stoeckius M, Hafemeister C, Stephenson W, Houck-Loomis B, Chattopadhyay PK, Swerdlow H, Satija R, Smibert P. Simultaneous epitope and transcriptome measurement in single cells. *Nat Methods* 2017; **14**:865–868.
 26. Cochain C, Vafadarnejad E, Arampatzi P, Pelisek J, Winkels H, Ley K, Wolf D, Saliba AE, Zerneck A. Single-cell RNA-Seq reveals the transcriptional landscape and heterogeneity of aortic macrophages in murine atherosclerosis. *Circ Res* 2018; **122**:1661–1674.
 27. Zerneck A, Winkels H, Cochain C, Williams JW, Wolf D, Soehnlein O, Robbins CS, Monaco C, Park I, McNamara CA, Binder CJ, Cybulsky MI, Scipione CA, Hedrick CC, Galkina EV, Kyaw T, Ghosh Y, Dinh HQ, Ley K. Meta-analysis of leukocyte diversity in atherosclerotic mouse aortas. *Circ Res* 2020; **127**:402–426.
 28. Newland SA, Mohanta S, Clement M, Taleb S, Walker JA, Nus M, Sage AP, Yin C, Hu D, Kitt LL, Finigan AJ, Rodewald HR, Binder CJ, McKenzie ANJ, Habenicht AJ, Mallat Z. Type-2 innate lymphoid cells control the development of atherosclerosis in mice. *Nat Commun* 2017; **8**:15781.
 29. Wu C, Chen Z, Xiao S, Thalhammer T, Madi A, Han T, Kuchroo V. SGK1 governs the reciprocal development of Th17 and regulatory T cells. *Cell Rep* 2018; **22**:653–665.
 30. Oppmann B, Lesley R, Blom B, Timans JC, Xu Y, Hunte B, Vega F, Yu N, Wang J, Singh K, Zonin F, Vaisberg E, Churakova T, Liu M, Gorman D, Wagner J, Zurawski S, Liu Y, Abrams JS, Moore KW, Rennick D, de Waal-Malefyt R, Hannum C, Bazan JF, Kastelein RA. Novel p19 protein engages IL-12p40 to form a cytokine, IL-23, with biological activities similar as well as distinct from IL-12. *Immunity* 2000; **13**:715–725.
 31. Pasparakis M, Vandenabeele P. Necroptosis and its role in inflammation. *Nature* 2015; **517**:311–320.
 32. Tan L, Sandroek I, Odak I, Aizenbud Y, Wilharm A, Barros-Martins J, Tabib Y, Borchers A, Amado T, Gangoda L, Herold MJ, Schmidt-Supprian M, Kisielow J, Silva-Santos B, Koenecke C, Hovav AH, Krebs C, Prinz I, Ravens S. Single-cell transcriptomics identifies the adaptation of Scart1(+) γ gamma6(+) T cells to skin residency as activated effector cells. *Cell Rep* 2019; **27**:3657–3671.e4.
 33. Riol-Blanco L, Lazarevic V, Awasthi A, Mitsdoerffer M, Wilson BS, Croxford A, Waisman A, Kuchroo VK, Glimcher LH, Oukka M. IL-23 receptor regulates unconventional IL-17-producing T cells that control bacterial infections. *J Immunol* 2010; **184**:1710–1720.
 34. Petrie EJ, Czabotar PE, Murphy JM. The structural basis of necroptotic cell death signaling. *Trends Biochem Sci* 2019; **44**:53–63.
 35. Karunakaran D, Nguyen MA, Geoffrion M, Vreeken D, Lister Z, Cheng HS, Otte N, Essebie P, Wyatt H, Kandiah JW, Jung R, Alenghat FJ, Mompeon A, Lee R, Pan C, Gordon E, Rasheed A, Lusic AJ, Liu P, Matic LP, Hedin U, Fish JE, Guo L, Kolodgie F, Virmani R, van Gils JM, Rayner KJ. RIPK1 expression associates with inflammation in early atherosclerosis in humans and can be therapeutically silenced to reduce NF-kappaB activation and atherogenesis in mice. *Circulation* 2021; **143**:163–177.
 36. Lin J, Li H, Yang M, Ren J, Huang Z, Han F, Huang J, Ma J, Zhang D, Zhang Z, Wu J, Huang D, Qiao M, Jin G, Wu Q, Huang Y, Du J, Han J. A role of RIP3-mediated macrophage necrosis in atherosclerosis development. *Cell Rep* 2013; **3**:200–210.
 37. Rasheed A, Robichaud S, Nguyen MA, Geoffrion M, Wyatt H, Cottee ML, Dennison T, Pietrangolo A, Lee R, Lagace TA, Ouimet M, Rayner KJ. Loss of MLKL (mixed lineage kinase domain-like protein) decreases necrotic core but increases macrophage lipid accumulation in atherosclerosis. *Arterioscler Thromb Vasc Biol* 2020; **40**:1155–1167.
 38. Carding SR, Egan PJ. Gammadelta T cells: functional plasticity and heterogeneity. *Nat Rev Immunol* 2002; **2**:336–345.
 39. Egan PJ, Carding SR. Downmodulation of the inflammatory response to bacterial infection by gammadelta T cells cytotoxic for activated macrophages. *J Exp Med* 2000; **191**:2145–2158.
 40. Komuczki J, Tuzlak S, Friebe E, Hartwig T, Spath S, Rosenstiel P, Waisman A, Opitz L, Oukka M, Schreiner B, Pelczar P, Becher B. Fate-mapping of GM-CSF expression identifies a discrete subset of inflammation-driving T helper cells regulated by cytokines IL-23 and IL-1beta. *Immunity* 2019; **50**:1289–1304.e6.
 41. Dwell P, Kono H, Rayner KJ, Sirois CM, Vladimer G, Bauernfeind FG, Abela GS, Franchi L, Nunez G, Schnurr M, Espevik T, Lien E, Fitzgerald KA, Rock KL, Moore KJ, Wright SD, Hornung V, Latz E. NLRP3 inflammasomes are required for atherogenesis and activated by cholesterol crystals. *Nature* 2010; **464**:1357–1361.
 42. Astry B, Venkatesha SH, Moudgil KD. Involvement of the IL-23/IL-17 axis and the Th17/Treg balance in the pathogenesis and control of autoimmune arthritis. *Cytokine* 2015; **74**:54–61.
 43. Izcue A, Hue S, Buonocore S, Arancibia-Carcamo CV, Ahern PP, Iwakura Y, Maloy KJ, Powrie F. Interleukin-23 restrains regulatory T cell activity to drive T cell-dependent colitis. *Immunity* 2008; **28**:559–570.
 44. Foks AC, Lichtman AH, Kuiper J. Treating atherosclerosis with regulatory T cells. *Arterioscler Thromb Vasc Biol* 2015; **35**:280–287.
 45. Weber C, Meiler S, Doring Y, Koch M, Drechsler M, Megens RT, Rowinska Z, Bidzhokov K, Fecher C, Ribechini E, van Zandvoort MA, Binder CJ, Jelinek I, Hristov M, Boon L, Jung S, Korn T, Lutz MB, Forster I, Zenke M, Hieronymus T, Junt T, Zerneck A. CCL17-expressing dendritic cells drive atherosclerosis by restraining regulatory T cell homeostasis in mice. *J Clin Invest* 2011; **121**:2898–2910.
 46. Choi JH, Do Y, Cheong C, Koh H, Boscardin SB, Oh YS, Bozzacco L, Trumpheller C, Park CG, Steinman RM. Identification of antigen-presenting dendritic cells in mouse aorta and cardiac valves. *J Exp Med* 2009; **206**:497–505.
 47. Heriaka M, Erridge C. High-fat meal induced postprandial inflammation. *Mol Nutr Food Res* 2014; **58**:136–146.
 48. Nus M, Sage AP, Lu Y, Masters L, Lam BYH, Newland S, Weller S, Tsiantoulas D, Raffort J, Marcus D, Finigan A, Kitt L, Figg N, Schirmbeck R, Kneilling M, Yeo GSH, Binder CJ, de la Pompa JL, Mallat Z. Marginal zone B cells control the response of follicular helper T cells to a high-cholesterol diet. *Nat Med* 2017; **23**:601–610.
 49. Tamassia N, Arruda-Silva F, Wright HL, Moots RJ, Gardiman E, Bianchetto-Aguilera F, Gasperini S, Capone M, Maggi L, Annunziato F, Edwards SW, Cassatella MA. Human neutrophils activated via TLR8 promote Th17 polarization through IL-23. *J Leukoc Biol* 2019; **105**:1155–1165.
 50. van Leeuwen M, Gijbels MJ, Duijvestijn A, Smook M, van de Gaar MJ, Heeringa P, de Winther MP, Tervaert JW. Accumulation of myeloperoxidase-positive neutrophils in atherosclerotic lesions in LDLR^{-/-} mice. *Arterioscler Thromb Vasc Biol* 2008; **28**:84–89.
 51. David A, Saitta S, De Caridi G, Benedetto F, Massara M, Risitano DC, Venuti FS, Spinelli F, Gangemi S. Interleukin-23 serum levels in patients affected by peripheral arterial disease. *Clin Biochem* 2012; **45**:275–278.
 52. Abbas A, Gregersen I, Holm S, Daissormont I, Bjerkeli V, Krohg-Sorensen K, Skagen KR, Dahl TB, Russell D, Almas T, Bundgaard D, Altheheld LH, Rashidi A, Dahl CP, Michelsen AE, Biessen EA, Aukrust P, Halvorsen B, Skjelland M. Interleukin 23 levels are increased in carotid atherosclerosis: possible role for the interleukin 23/interleukin 17 axis. *Stroke* 2015; **46**:793–799.
 53. Stefanadis C, Antoniou CK, Tsiachris D, Pietri P. Coronary atherosclerotic vulnerable plaque: current perspectives. *J Am Heart Assoc* 2017; **6**:e005543.
 54. Espigol-Frigole G, Planas-Rigol E, Ohnuki H, Salvucci O, Kwak H, Ravichandran S, Luke B, Cid MC, Tosato G. Identification of IL-23p19 as an endothelial proinflammatory peptide that promotes gp130-STAT3 signaling. *Sci Signal* 2016; **9**:ra28.
 55. Conway R, O'Neill L, Gallagher P, McCarthy GM, Murphy CC, Veale DJ, Fearon U, Molloy ES. Ustekinumab for refractory giant cell arteritis: a prospective 52-week trial. *Semin Arthritis Rheum* 2018; **48**:523–528.

Translational perspective

The mechanisms and cell types contributing to early inflammation and lesion formation are incompletely understood. Here, we demonstrate that the aortic root harbours a population of IL23R-dependent $\gamma\delta$ T cells that can release IL-17 and GM-CSF, and both cytokines together induce macrophage inflammation and necroptosis. IL-23R⁺ $\gamma\delta$ T cells locally promote early lesion formation in the aortic root and contribute to the expansion of the necrotic core, a hallmark of vulnerable atherosclerotic lesions. Targeting IL-23R or IL-23 itself could thus be further explored as a therapeutic option in atherosclerosis.